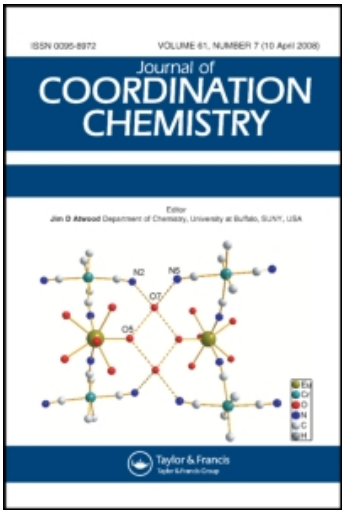

Journal of Coordination Chemistry
Publication details, including instructions for authors and subscription information:
http://www.informaworld.com/smpp/title~content=t713455674

Syntheses, structures, and magnetic properties of dinuclear/1-D copper(II) acetato and formato derivatives with methylpyrazine and dimethylpyrazine

Montserrat Barquín[a]; María J. González Garmendia[a]; Liher Larrínaga[a]; Elena Pinilla[bc]; José M. Seco[a]; María R. Torres[b]
[a] Facultad de Ciencias Químicas, Grupo de Química Inorgánica, Universidad del País Vasco, Spain [b] Facultad de Ciencias Químicas, Laboratorio de Difracción de Rayos X, Universidad Complutense, 28040 Madrid, Spain [c] Facultad de Ciencias Químicas, Departamento de Química Inorgánica, Universidad Complutense, 28040 Madrid, Spain

First published on: 11 June 2010

To cite this Article Barquín, Montserrat , González Garmendia, María J. , Larrínaga, Liher , Pinilla, Elena , Seco, José M. and Torres, María R.(2010) 'Syntheses, structures, and magnetic properties of dinuclear/1-D copper(II) acetato and formato derivatives with methylpyrazine and dimethylpyrazine', Journal of Coordination Chemistry, 63: 10, 1652 — 1665, First published on: 11 June 2010 (iFirst)
To link to this Article: DOI: 10.1080/00958972.2010.487559
URL: http://dx.doi.org/10.1080/00958972.2010.487559

Journal of Coordination Chemistry
Vol. 63, No. 10, 20 May 2010, 1652–1665

Syntheses, structures, and magnetic properties of dinuclear/1-D copper(II) acetato and formato derivatives with methylpyrazine and dimethylpyrazine

MONTSERRAT BARQUÍN*†, MARÍA J. GONZÁLEZ GARMENDIA†, LIHER LARRÍNAGA†, ELENA PINILLA‡§, JOSÉ M. SECO† and MARÍA R. TORRES‡

†Facultad de Ciencias Químicas, Grupo de Química Inorgánica, Universidad del País Vasco, UPV/EHU, Apartado 1072, 20080 San Sebastián, Spain
‡Facultad de Ciencias Químicas, Laboratorio de Difracción de Rayos X, Universidad Complutense, 28040 Madrid, Spain
§Facultad de Ciencias Químicas, Departamento de Química Inorgánica, Universidad Complutense, 28040 Madrid, Spain

(*Received 27 November 2009; in final form 11 March 2010*)

In this study, $\{[Cu_2(\mu\text{-}HCO_2)_4](\mu\text{-Mepyrz})\}_n$ (**1**), $[Cu_2(\mu\text{-}HCO_2)_4(Mepyrz)_2]$ (**2**), $\{[Cu_2(\mu\text{-AcO})_4](\mu\text{-Mepyrz})\}_n$ (**3**), $[Cu_2(\mu\text{-AcO})_4(Mepyrz)_2]$ (**4**), $[Cu_2(\mu\text{-AcO})_4(2,3\text{-Me}_2\text{pyrz})_2]$ (**5**), $[Cu_2(\mu\text{-AcO})_4(2,6\text{-Me}_2\text{pyrz})_2]$ (**6**), and $\{[Cu_2(\mu\text{-AcO})_4](\mu\text{-}2,5\text{-Me}_2\text{pyrz})\}_n$ (**7**) have been synthesized and characterized by chemical analysis and electronic spectroscopy. Compounds **2**, **4**, **5**, and **6**, characterized by single-crystal X-ray diffraction, are composed of molecular dimers based on a *paddle-wheel* motif with two coppers, four *syn–syn* carboxylates, and two ligands coordinated to copper in the axial positions. In **7**, chains of $[Cu_2(\mu\text{-AcO})_4]$ dimers with 2,5-Me_2pyrz as bridging ligands are formed. Magnetic properties and electron paramagnetic resonance results of the compounds are also described.

Keywords: Copper; Methylpyrazine; Dimethylpyrazine; Dimers; Chain of dimers

1. Introduction

The dinuclear copper acetate dihydrate complex, $[Cu_2(\mu\text{-OAc})_4(H_2O)_2]$ and its adducts $[Cu_2(\mu\text{-OAc})_4L_2]$ with different ligands in the axial positions, are amongst the most studied dinuclear compounds of Cu(II) in their structural and magnetic aspects [1–6]. On the contrary, few compounds containing the *paddle-wheel* dinuclear group $[Cu_2(\mu\text{-}HCO_2)_4]$, with four *syn–syn* formate groups are known. This structure is present in different types of complexes: molecular dimers as $[Cu_2(\mu\text{-HCOO})_4(urea)_2]$ [7], $[Cu_2(\mu\text{-HCOO})_4(DMSO)_2]$ [8], and $[Cu_2(\mu\text{-HCOO})_4(DMF)_2]$ [9], or chains of dimers as $\cdots$dioxane–$[Cu_2(\mu\text{-HCOO})_4]$–dioxane–$[Cu_2(\mu\text{-HCOO})_4]$–$\cdots$ [10].

*Corresponding author. Email: montserrat.barquin@ehu.es

ISSN 0095-8972 print/ISSN 1029-0389 online
DOI: 10.1080/00958972.2010.487559

Previously, we reported complexes with 2-(phenylamino)pyridine and 2-(methylamino)pyridine, $[Cu_2(\mu\text{-}OAc)_4(PhNHpy)_2]$ [11], $[Cu_2(\mu\text{-}OAc)_4(MeNHpy)_2]$ [12], and $[Cu_2(\mu\text{-}HCO_2)_4(PhNHpy)_2]$ and $[Cu_2(\mu\text{-}HCO_2)_4(MeNHpy)_2]$ [13]. In all the cases, the structural and magnetic results were similar to those of the copper acetate hydrate. The ligands are coordinated in the axial positions of the dimer through the pyridinic nitrogen. Two intramolecular hydrogen bonds are formed between each ligand and an oxygen of one acetate. Compounds containing dimeric *paddle-wheel* copper(II) units with diverse carboxylate and dicarboxylate groups receive much attention [14, 15].

Pyrazine, NC_4H_4N (pyrz), is a ligand which can be monodentate or, more frequently, bidentate [16]. In the last case, pyrazine is a very suitable ligand for forming coordination polymers. The copper acetate $[Cu_2(\mu\text{-}AcO)_4(H_2O)_2]$ forms a linear-chain complex $[Cu_2(\mu\text{-}AcO)_4(\mu\text{-}pyrz)]_n$, a chain of dimers, in which binuclear copper acetate units are linked by pyrazine bridges [17, 18].

In a previous paper, we described the interaction between $Cu(HCO_2)_2 \cdot 4H_2O$ and pyrazine, and the different isomers of dimethylpyrazine. Two compounds were obtained with pyrazine, $Cu(HCO_2)_2(pyrz)$ (3-D) and $Cu_2(HCO_2)_4(pyrz)$ (chain of dimers). A chain of dimers was obtained with 2,3-dimethylpyrazine $Cu_2(HCO_2)_4(2,3\text{-}Me_2pyrz)$. The 2,6-dimethylpyrazine is monodentate because of the relative position of the methyl groups and $[Cu_2(\mu\text{-}HCO_2)_4(2,6\text{-}Me_2pyrz)_2]$ was formed [19].

In this study, we describe the interaction between $Cu(HCO_2)_2 \cdot 4H_2O$ and Mepyrz, and the interaction between $Cu(AcO)_2 \cdot H_2O$ and Mepyrz, 2,3-Me_2pyrz, 2,5-Me_2pyrz, and 2,6-Me_2pyrz. Magnetic properties and electron paramagnetic resonance (EPR) spectra are also studied.

2. Experimental

2.1. *Physical measurements*

C, H, and N analyses were carried out using a Leco 932-CHNS microanalyzer. Infrared (IR) spectra were recorded with a Nicolet FT-IR 510 spectrometer from 4000 to 400 cm^{-1} using KBr pellets. Electronic spectra were recorded with a Shimadzu UV-265 FW spectrophotometer. Magnetic measurements were carried out using a Quantum Design SQUID MPMSXL magnetometer with an applied field of 10,000 G. Diamagnetic corrections were applied [20]. A correction for temperature-independent paramagnetism (TIP) of 60×10^{-6} cm^3 mol^{-1} per mol of Cu was applied in all the cases. The EPR spectra were recorded on a Bruker ESP 300 spectrometer with a Bruker ER 035 gaussmeter and an HP 5325 frequency counter, for powder samples, in Q band, at 120 K.

2.2. *Synthesis*

2.2.1. Synthesis of 1 and 2

$\{[Cu_2(\mu\text{-}HCO_2)_4](\mu\text{-}Mepyrz)\}_n$ (1): The complex was prepared by the addition of solid $Cu(HCOO)_2 \cdot 4H_2O$ (226 mg, 1 mmol) to a solution of methylpyrazine (0.045 mL, 0.5 mmol) in methanol: chloroform 1 : 3 (10 mL). The mixture was stirred overnight and

evaporated to dryness in a rotary evaporator. The solid was treated with CCl_4, filtered, washed with CCl_4, and dried *in vacuo* over $CaCl_2$. Yield: 161 mg, 80%. Anal. Calcd for $C_9Cu_2H_{10}N_2O_8$ (%): C, 26.94; H, 2.51; and N, 6.98. Found (%): C, 26.90; H, 2.49; and N, 6.99. IR (KBr; cm^{-1}): 1628(vs), 1577(sh), 1485(s), 1372(m), 1352(s), 1078(m), 1039(m), 830(m), and 775(m).

Despite using different molar proportions of $Cu(HCOO)_2 \cdot 4H_2O$ and Mepyrz (1 : 0.5, 1 : 1, and 1 : 2), only $Cu_2(HCOO)_4$(Mepyrz), as powder, was obtained.

[Cu_2(μ-HCO_2)$_4$(Mepyrz)$_2$] (2): Crystals suitable for X-ray diffraction were obtained by slow evaporation of the solvent from a solution of $Cu(HCOO)_2 \cdot 4H_2O$ and Mepyrz in MeCN in a molar proportion 1 : 0.5.

2.2.2. Synthesis of 3 and 4

{[Cu_2(μ-AcO)$_4$](μ-Mepyrz)}$_n$ (3): The complex was prepared by the addition of solid $Cu(AcO)_2 \cdot H_2O$ (200 mg, 1 mmol) to a solution of methylpyrazine (0.182 mL, 2 mmol) in MeCN (20 mL). The mixture was stirred overnight. The green precipitate formed was filtered off, washed with MeCN and Et_2O, and dried *in vacuo* over $CaCl_2$. Yield: 186 mg, 81%. Anal. Calcd for $C_{13}Cu_2H_{18}N_2O_8$ (%): C, 34.14; H, 3.97; and N, 6.12. Found (%): C, 34.13; H, 3.97; and N, 6.20. IR (KBr; cm^{-1}): 1610(vs), 1442(s), 1420(s), 1348(m), 1075(m), 1034(m), 842(m), and 684(m).

Although different molar proportions of $Cu(AcO)_2 \cdot H_2O$ and Me-pyrazine (1 : 0.5, 1 : 1, and 1 : 2) were used, only $Cu_2(AcO)_4$(Mepyrz), as powder, was obtained.

[Cu_2(μ-AcO)$_4$(Mepyrz)$_2$] (4): Crystals suitable for X-ray diffraction were obtained by slow evaporation of the filtrate in the synthesis of **3**.

2.2.3. Synthesis of [Cu_2(μ-AcO)$_4$(2,3-Me_2pyrz)$_2$] (5). 2,3-Me_2pyrz (0.423 mL, 4 mmol) was added to a solution of $Cu(AcO)_2 \cdot H_2O$ (199 mg, 1 mmol) in MeOH (30 mL). The green solution was stirred for 30 min at room temperature. After slow evaporation of solvent, a green precipitate and crystals suitable for X-ray diffraction were formed. Yield: 154 mg, 53%. Anal. Calcd for $C_{20}Cu_2H_{28}N_4O_8$ (%): C, 41.45; H, 4.87; and N, 9.67. Found (%): C, 41.71; H, 4.80; and N, 9.70. IR (KBr; cm^{-1}): 1628(vs), 1430(s), 1403(m), 1348(m), 1174(m), 1024(w), 859(m), and 627(m).

2.2.4. Synthesis of [Cu_2(μ-AcO)$_4$(2,6-Me_2pyrz)$_2$] (6). 2,6-Me_2pyrz (0.433 mL, 4 mmol) was added to a solution of $Cu(AcO)_2 \cdot H_2O$ (199 mg, 1 mmol) in MeCN (30 mL). The mixture was stirred for 5 h. The green precipitate formed was filtered off, washed with MeCN, and Et_2O and dried *in vacuo* over $CaCl_2$. Yield: 162 mg, 56%. Anal. Calcd for $C_{20}Cu_2H_{28}N_4O_8$ (%): C, 41.45; H, 4.87; and N, 9.67. Found (%): C, 41.47; H, 4.86; and N, 9.72. IR (KBr; cm^{-1}): 1620(vs), 1533(m), 1420(s), 1380(m), 1346(m), 1165(m), 1020(m), 881(m), and 684(m). Crystals suitable for X-ray diffraction were obtained by slow evaporation of the filtrate.

2.2.5. Synthesis of {[Cu_2(μ-AcO)$_4$](μ-2,5-Me_2pyrz)}$_n$ (7). 2,5-Me_2pyrz (0.436 mL, 4 mmol) was added to a solution of $Cu(AcO)_2 \cdot H_2O$ (199 mg, 1 mmol) in MeCN (30 mL) and stirred for 5 h. The green precipitate formed was filtered off, washed with MeCN and Et_2O, and dried *in vacuo* over $CaCl_2$. Yield: 169 mg, 72%. Anal. Calcd for

$C_{14}Cu_2H_{20}N_2O_8$ (%): C, 35.67; H, 4.28; and N, 5.94. Found (%): C, 35.77; H, 4.27; and N, 5.96. IR (KBr; cm^{-1}): 1617(vs), 1499(m), 1431(s), 1336(m), 1066(m), 850(m), and 684(m). Crystals suitable for X-ray diffraction were obtained by slow evaporation of the filtrate.

2.3. *X-ray crystallographic study*

Data collection was carried out at room temperature on a Bruker Smart CCD diffractometer using graphite-monochromated Mo-Kα radiation ($\lambda = 0.71073$ Å), operating at 50 kV and 35 mA for **2** and **7**, and at 50 kV and 25 mA for **4**, **5**, and **6**, respectively. In all the cases, data were collected over a hemisphere of the reciprocal space by a combination of three exposure sets. Each exposure was of 30 or 20 s and covered 0.3° in ω. The first 50 frames were recollected at the end of the data collection to monitor crystal decay, and no appreciable decay was observed.

A summary of the fundamental crystal and refinement data is given in table 1. The structures were solved by direct methods and refined by full-matrix least-square procedures on F^2 [21]. All non-hydrogen atoms were refined anisotropically, and all hydrogens were included in the calculated positions and refined riding on the respective carbons.

3. Results and discussion

3.1. *Synthesis and characterization*

Compounds **1** and **3** were obtained by reactions of Mepyrz with $Cu(AcO)_2 \cdot H_2O$ or $Cu(HCO_2)_2 \cdot 4H_2O$ using molar proportions of copper carboxylate and ligands 1 : 0.5; 1 : 1, or 1 : 2. Crystals suitable for X-ray diffraction were obtained only with the composition 1 : 1 (**2** and **4**).

With 2,3- and 2,6-Me_2pyrz, an excess of ligand in proportion 1 : 4 is required to obtain complexes with 1 : 1 ratio, **5** and **6**. With $Cu(AcO)_2 \cdot H_2O$ and 2,5-Me_2pyrz in all the tested proportions (1 : 0.5, 1 : 1, 1 : 2, and 1 : 4), compound **7** was formed.

In the visible region of the diffuse reflectance spectra of the complexes, a broad band assigned to d–d transitions is observed centered at 680–700 nm. The absorption at 380 nm, characteristic of the $[Cu_2(\mu\text{-}RCOO)_4]$ group, is also observed. At 250–290 nm, two ligand transitions are observed in all the cases.

3.2. *Description of the structures*

3.2.1. Crystal structure of 2. The crystal structure consists of two crystallographically independent centrosymmetric dimeric molecules with a Mepyrz molecule coordinated to each copper in the $[Cu_2(\mu\text{-}HCO_2)_4]$ unit (figure 1). There are some slight differences between both the molecules, related to the relative disposition of the methylpyrazine ring. Thus, the values of the dihedral angles between methylpyrazine ring N1C1C2N2C3C4 and the best least-square planes Cu1O3C5O1′Cu1′O3′C5′O1 and Cu1O2C9′O4′Cu1′O2′C9O4 are 69.4(1)° and 25.4(1)°, respectively, whereas between the

Table 1. Crystal data and structure refinement for **2** and **4**–**7**.

	2	**4**	**5**	**6**	**7**
Empirical formula	$C_{14}H_{16}N_4O_8Cu_2$	$C_{18}H_{24}N_4O_8Cu_2$	$C_{20}H_{28}N_4O_8Cu_2$	$C_{20}H_{28}N_4O_8Cu_2$	$C_7H_{10}NO_4Cu$
Formula weight	495.39	551.49	579.54	579.54	235.70
Crystal system	Triclinic	Triclinic	Monoclinic	Monoclinic	Monoclinic
Space group	$P\bar{1}$	$P\bar{1}$	$P2(1)/c$	$P2(1)/n$	$P2(1)/n$
Unit cell dimensions (Å, °)					
a	7.0388(8)	7.378(1)	10.0231(8)	11.7404(9)	8.5487(7)
b	10.415(1)	8.575(1)	15.248(1)	8.0562(6)	12.268(1)
c	13.546(2)	9.774(1)	8.1082(7)	14.097(1)	9.8038(8)
α	89.320(2)	97.186(3)			
β	82.952(2)	109.041(2)	97.493(2)	110.237(1)	107.325(2)
γ	71.854(2)	97.762(2)			
Volume (Å^3), Z	936.2(2), 2	569.6(1), 1	1228.6(2), 2	1251.0(2), 2	981.5(1), 4
Calculated density (mg m^{-3})	1.757	1.608	1.567	1.539	1.595
Absorption coefficient (mm^{-1})	2.322	1.917	1.782	1.750	2.207
Scan technique	ω and φ	ω and φ	ω and φ	ω and φ	ω and φ
$F(000)$	500	282	596	596	480
θ range for data collection (°)	1.52–26.00	2.24–26.00	2.05–26.00	1.95–26.00	2.74–26.00
Index ranges	From $(-8, -12, -10)$ to $(8, 12, 16)$	From $(-8, -8, -12)$ to $(9, 10, 8)$	From $(-8, -18, -16)$ to $(12, 16, 8)$	From $(-14, -9, -11)$ to $(14, 9, 17)$	From $(-10, -13, -15)$ to $(8, 15, 11)$
Reflections collected	5352	3169	6722	6756	5322
Independent reflections	3603 [R(int) = 0.0503]	2160 [R(int) = 0.0560]	2390 [R(int) = 0.0475]	2448 [R(int) = 0.0479]	1910 [R(int) = 0.0619]
Completeness to θ (%)	98.0	97.2	99.4	99.7	91.9
Data/restraints/parameters	3603/0/253	2160/0/145	2390/0/154	2448/0/154	1910/0/118
Goodness-of-fit on F^2	0.867	1.056	1.043	0.980	1.098
R^a (reflections observed) [$I > 2\sigma(I)$]	0.0415 (2147)	0.0371 (1909)	0.0296 (1969)	0.0293 (1855)	0.0361 (1590)
$Rw_F{}^b$ (all data)	0.0846	0.1012	0.0845	0.0747	0.0925
Largest difference peak and hole (e Å^{-3})	0.465 and −0.338	0.709 and −0.495	0.261 and −0.307	0.364 and −0.170	0.390 and −0.827

[a] $\sum||F_o| - |F_c||/\sum|F_o|$.

[b] $\{\sum[w(F_o^2 - F_c^2)^2]/\sum[w(F_o^2)^2]\}^{1/2}$.

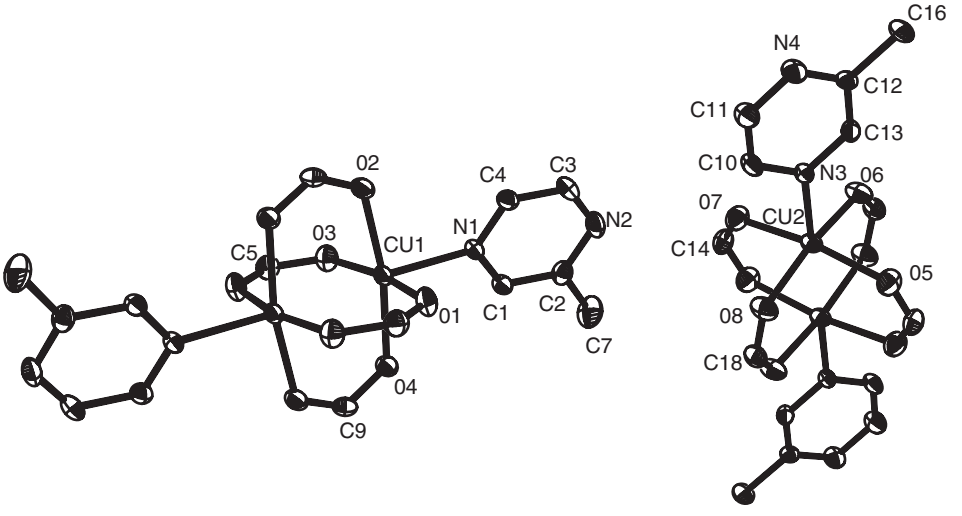

Figure 1. ORTEP view (25% of probability) of dimeric molecules in **2** showing the atomic numbering of the asymmetric unit. The hydrogen atoms have been omitted for clarity.

Table 2. Selected interatomic distances (Å) and angles (°) for **2**.

Cu1–O1	1.983(3)	Cu2–O5	1.967(4)
Cu1–O2	1.969(3)	Cu2–O6	1.963(3)
Cu1–O3	1.962(3)	Cu2–O7	1.975(4)
Cu1–O4	1.975(3)	Cu2–O8	1.965(3)
Cu1–N1	2.181(3)	Cu2–N3	2.150(3)
Cu1···Cu1$^{\#1}$	2.654(1)	Cu2···Cu2$^{\#2}$	2.671(1)
O1–Cu1–O2	89.4(1)	O5–Cu2–O6	88.5(2)
O1–Cu1–O3	167.9(1)	O5–Cu2–O7	167.2(1)
O1–Cu1–O4	89.5(1)	O5–Cu2–O8	89.6(2)
O2–Cu1–O3	90.3(1)	O6–Cu2–O7	90.5(2)
O2–Cu1–O4	168.3(1)	O6–Cu2–O8	167.3(1)
O3–Cu1–O4	88.3(1)	O7–Cu2–O8	88.6(2)
N1–Cu1–O1	92.4(1)	N3–Cu2–O5	99.0(1)
N1–Cu1–O2	96.9(1)	N3–Cu2–O6	94.4(1)
N1–Cu1–O3	99.7(1)	N3–Cu2–O7	93.8(1)
N1–Cu1–O4	94.7(1)	N3–Cu2–O8	98.3(1)
N1–Cu1···Cu1$^{\#1}$	173.8(1)	N3–Cu2···Cu2$^{\#2}$	175.7(1)

Symmetry transformations used to generate equivalent atoms: $^{\#1}-x, -y+2, -z+2$; $^{\#2}-x+1, -y, -z+1$.

methylpyrazine ring N3C10C11N4C12C13 and the best least-square planes Cu2O7C14O5′Cu2′O7′C14′O5 and Cu2O8C18O6′Cu2′O8′C18′O6 are 55.7(1)° and 34.3(1)°, respectively. Selected interatomic distances and angles are given in table 2.

Each Cu exhibits a square-pyramidal geometry. The trigonality indices [22] deduced from the angles data, $\tau = 0.007$ for Cu1 and 0.0003 for Cu2, indicate square-pyramidal geometry. The copper rises from the basal plane to the apical nitrogen by 0.204(1) Å for Cu1 and 0.219(1) Å for Cu2. The two independent dimers have different orientations in the crystal. Rows of dimers of the same orientation are observed along *a*- and *b*-axis, and they form sheets parallel to the *ab* plane (figure 2).

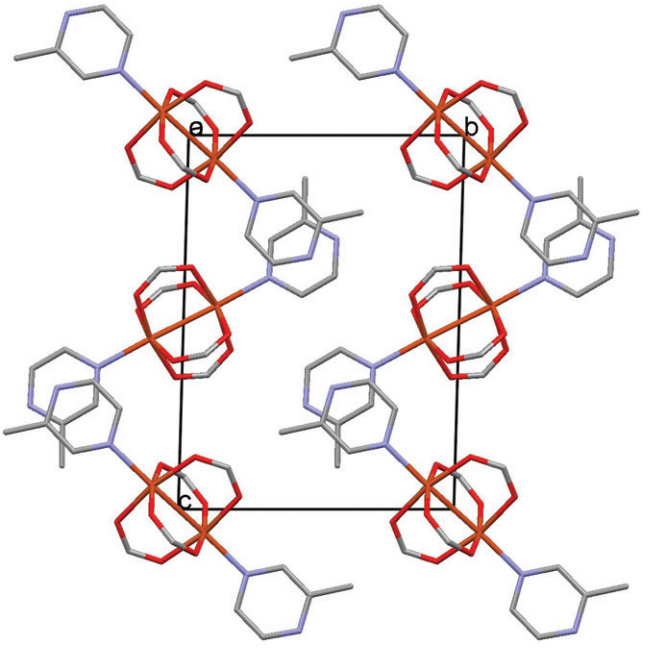

Figure 2. Dimer disposition in the crystal of **2** viewed along the *a*-axis.

3.2.2. Crystal structure of 4–6. The crystal structures of these complexes consist of centrosymmetric dimers. The Oak Ridge Thermal Ellipsoid Plot Program (ORTEP) view for **5** is shown in figure 3. Selected interatomic distances and angles for **4–6** are given in table 3.

The trigonality indices [22] $\tau = 0.002$, 0.005, and 0.002 for **4**, **5**, and **6**, respectively, correspond to square-pyramidal geometry. The copper rises from the basal plane to the apical nitrogen by 0.192(1) Å for **4**, 0.2152(9) Å for **5**, and 0.1891(9) Å for **6**. The distances Cu–N1 are shorter in **4** and **6** than in **5** (table 3), due to the disposition of the methyl in the dimethylpyrazine rings in *ortho* with respect to the nitrogen in **5**, which is closer to the methyl group of the acetate than in **4** and **6**.

Disposition of the dimers in the crystal is shown in figure 4; in **4** (figure 4a) all the dimers have the same orientation in the crystal while in **5** (figure 4b) and **6** (figure 4c), they have two orientations, as in **2**.

3.2.3. Crystal structure of 7. This structure consists of polymeric chains, parallel to the *c*-axis, of $[Cu_2(\mu\text{-AcO})_4]$ units bridged by 2,5-Me_2pyrz molecules. Figure 5(a) shows the polymeric chain with atomic numbering of the asymmetric unit. Table 4 gives the selected interatomic distances and bond angles for **7**.

The trigonality index [22] $\tau = 0.004$ corresponds to a square pyramid with copper above the basal plane by 0.200(2) Å.

Figure 5(b) shows packing in **7** along *a*-axis. The methyl group of the acetate group is oriented toward the methylpyrazine of neighboring chains, reinforcing the crystal packing (the distance between the carbon of acetate and the ring centroid is 3.566 Å).

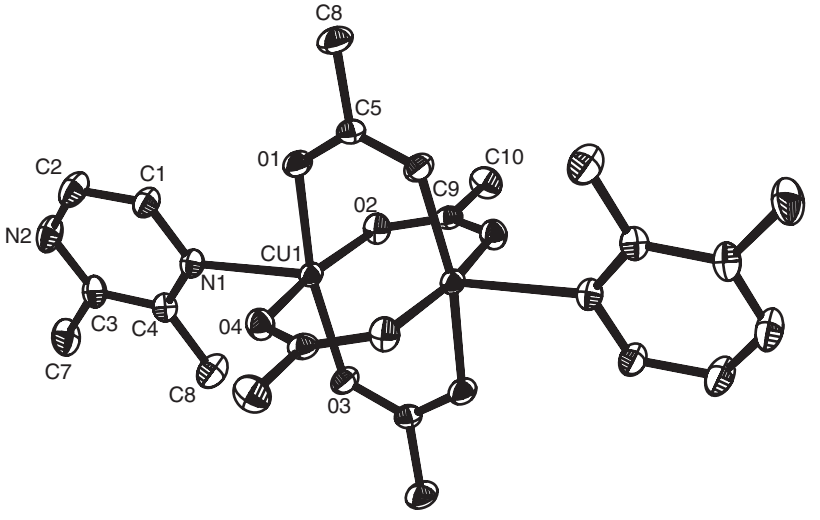

Figure 3. ORTEP view of dimeric molecule in **5** showing the atomic numbering of the asymmetric unit. The hydrogen atoms have been omitted for clarity.

Table 3. Selected interatomic distances (Å) and angles (°) for **4**–**6**.

	4	**5**	**6**
Cu1–O1	1.967(2)	1.975(2)	1.966(2)
Cu1–O2	1.964(2)	1.962(2)	1.963(2)
Cu1–O3	1.972(2)	1.961(2)	1.970(2)
Cu1–O4	1.967(2)	1.971(2)	1.970(2)
Cu1–N1	2.202(2)	2.326(2)	2.204(2)
Cu1···Cu1$^{\#1}$	2.614(1)	2.659(1)	2.609(1)
O1–Cu1–O2	88.9(1)	89.3(1)	89.6(1)
O1–Cu1–O3	168.6(1)	167.2(1)	168.9(1)
O1–Cu1–O4	90.8(1)	88.7(1)	88.8(1)
O2–Cu1–O3	88.8(1)	89.7(1)	89.3(1)
O2–Cu1–O4	168.5(1)	167.6(1)	169.0(1)
O3–Cu1–O4	89.37(1)	89.5(1)	90.2(1)
N1–Cu1–O1	97.3(1)	91.7(1)	94.9(1)
N1–Cu1–O2	96.8(1)	97.8(1)	96.4(1)
N1–Cu1–O3	94.0(1)	101.0(1)	96.2(1)
N1–Cu1–O4	94.6(8)	94.5(1)	94.6(1)
N1–Cu1···Cu1$^{\#1}$	176.8(1)	176.4(1)	178.4(1)

Symmetry transformations used to generate equivalent atoms $^{\#1}$: **4** and **6**, $-x+1$, $-y+1$, $-z$; **5**, $-x$, $-y$, $-z+1$.

3.3. *Magnetic and EPR results*

The quantities of **2** and **4** obtained were not enough to make magnetic and EPR measurements.

Compounds **1**, **3**, **5**, **6**, and **7** show strong antiferromagnetism, characteristic of the dimeric [Cu_2(μ-RCOO)$_4$] groups. The $\chi_M T$ values decrease with decreasing temperature for all these compounds. Figure 6 shows the plot of $\chi_M T$, per mol of dimer, *versus* temperature (T) for **5**. The results are similar to other compounds containing

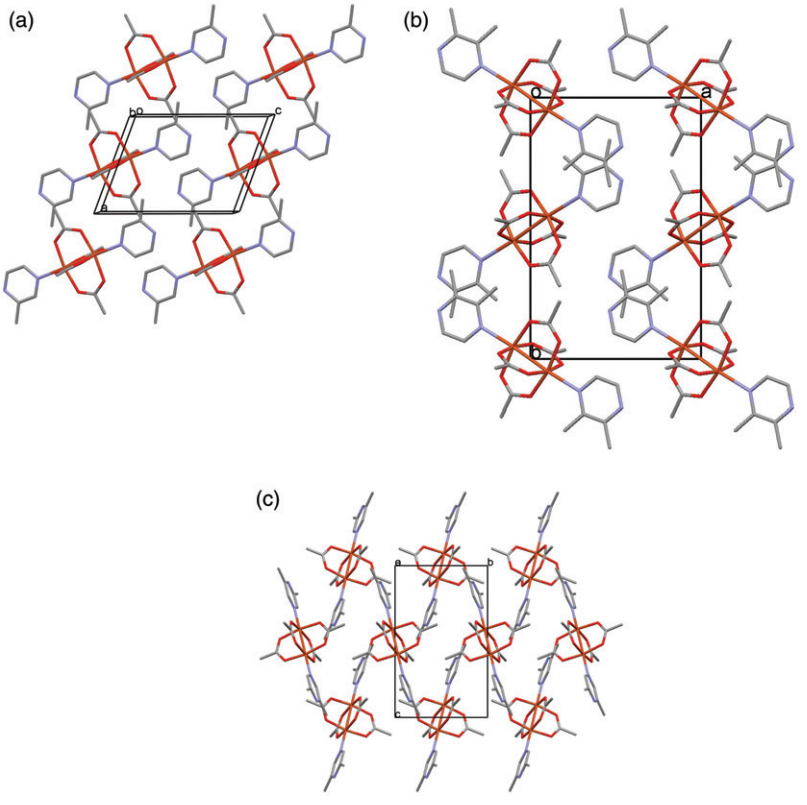

Figure 4. View of the crystal along the *a*-axis in (a) **4**; (b) **5**; and (c) **6**.

paddle-wheel copper units. The possible interdimer interaction in **1**, **3**, and **7** are negligible compared to the intradimer interaction [17].

The data from 50 to 300 K were fitted to the Bleaney–Bowers equation for a dimer with $S_1 = S_2 = ½$ [23]:

$$\chi_M(\mathrm{Cu}) = [(Ng^2\beta^2/kT)\,e^{(2J/kT)}/(1 + 3\,e^{(2J/kT)})] + N\alpha$$

where $2J$ is the separation between singlet and triplet states and $N\alpha$ is the TIP. The best fit for $g = 2.14$ (EPR result) and $N\alpha = 60 \times 10^{-6}\,\mathrm{cm^3 mol^{-1}}$ are given in table 5 along with the magnetic moments at 120 K.

These results indicate the presence of dimeric groups in **1** and **3**, even though their crystal structures are unknown. These results, together with the composition of these compounds, suggest a chain structure for **1** and **3**, similar to that of **7**. The antiferromagnetic parameter, $2J$, is the highest for **1**, the complex of the $[Cu_2(\mu\text{-}HCO_2)_4]$ group. This result agrees with the conclusions of Rodríguez-Fortea *et al*. [24] in a density functional study of the exchange coupling in carboxylato-bridged dinuclear copper(II) compounds; in $[Cu_2(\mu\text{-}RCOO)_4]$ groups, the antiferromagnetic interaction strength decreases with the presence of electron-withdrawing *R* groups. This explains the diference between $2J$ values for acetato and formato derivative.

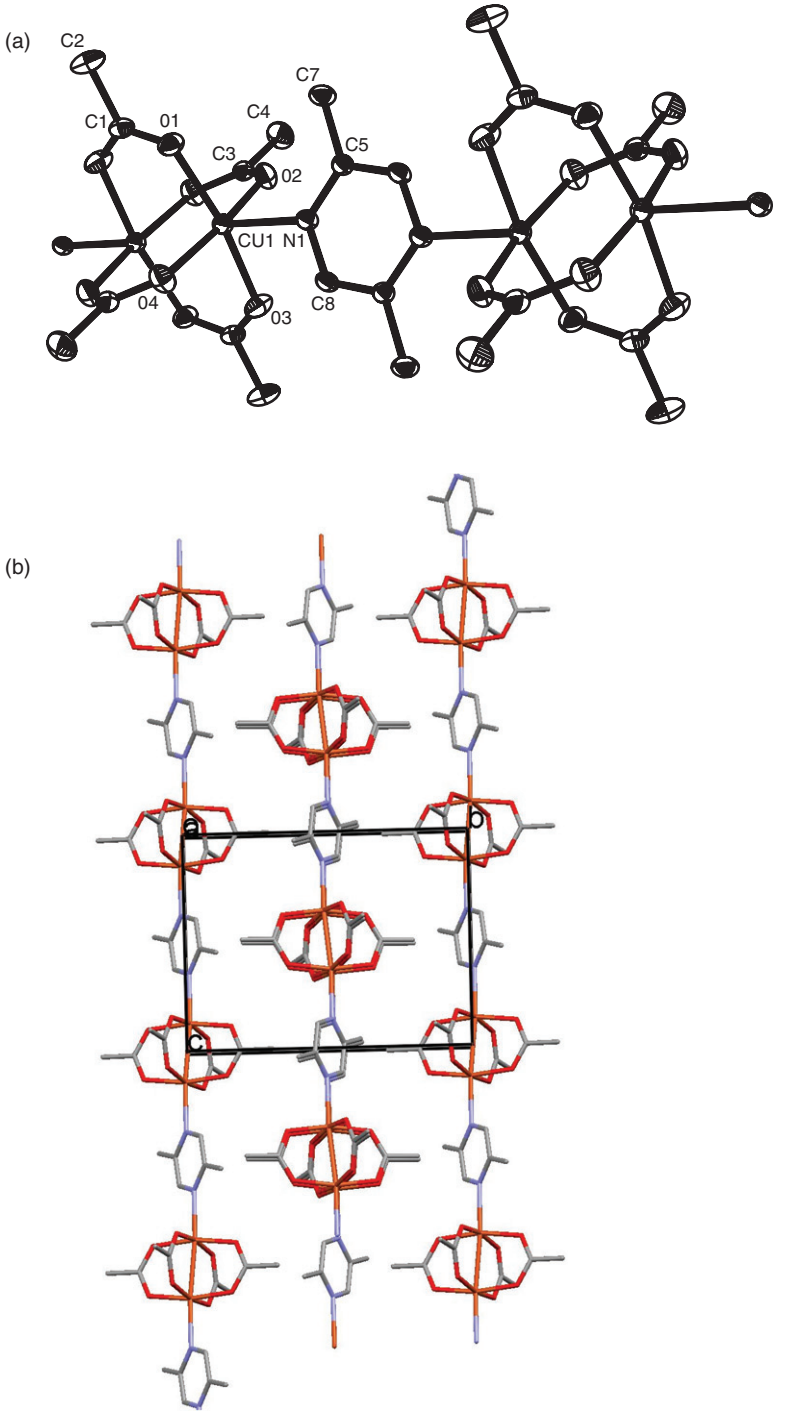

Figure 5. (a) ORTEP view of polymeric chain of **7** showing the atomic numbering of the asymmetric unit. The hydrogen atoms have been omitted for clarity; (b) view of **7** along the *a*-axis.

Table 4. Selected interatomic distances (Å) and angles (°) for **7**.

Cu1–O1	1.956(2)	O1–Cu1–O2	89.8(1)
Cu1–O2	1.965(2)	O1–Cu1–O3	168.4(1)
Cu1–O3	1.971(2)	O1–Cu1–O4	89.2(1)
Cu1–O4	1.973(2)	O2–Cu1–O3	90.4(1)
Cu1–N1	2.236(2)	O2–Cu1–O4	168.6(1)
Cu1···Cu1$^{\#1}$	2.616(1)	O3–Cu1–O4	88.4(1)
		N1–Cu1–O1	101.2(1)
		N1–Cu1–O2	97.9(1)
		N1–Cu1–O3	90.3(1)
		N1–Cu1–O4	93.5(1)
		N1–Cu1···Cu1$^{\#1}$	173.3(1)
		Cu1–N1···N1$^{\#2}$	171.2(4)

Symmetry transformations used to generate equivalent atoms: $^{\#1}-x, -y+1, -z+1$; $^{\#2}-x, -y+1, -z+2$.

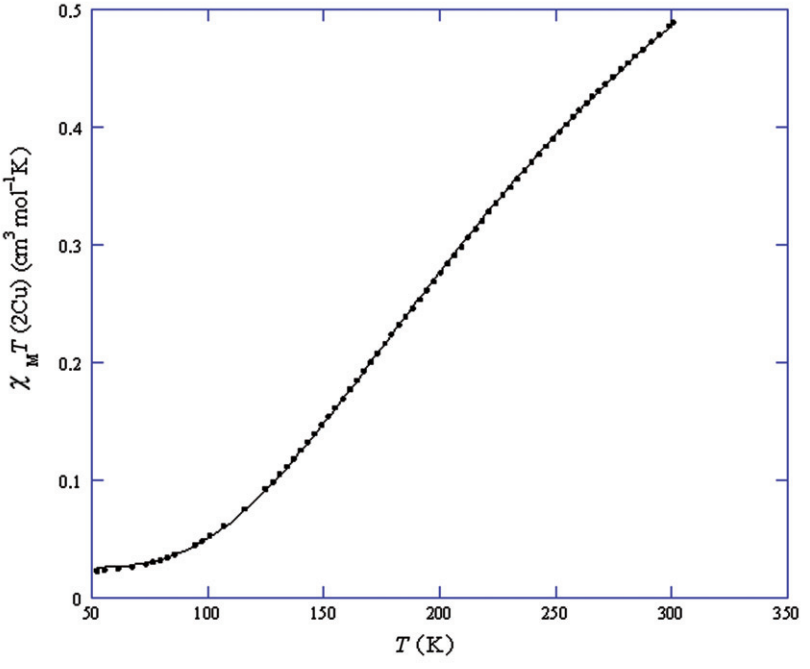

Figure 6. Plot of $\chi_M T$ *vs.* T, per mol of dimer, for **5**.

Table 5. Magnetic results.

Compound	$2J$ (cm^{-1})	R	μ (B.M.) (2Cu, 120 K)
1	−363	9.7×10^{-5}	1.20
3	−316	8.6×10^{-4}	0.85
5	−320	7.1×10^{-5}	0.81
6	−284	1.8×10^{-5}	1.05
7	−276	2.9×10^{-5}	1.09

$R = \Sigma(\chi_M T_{iexp} - \chi_M T_{ical})^2 / \Sigma(\chi_M T_{iexp})^2$.

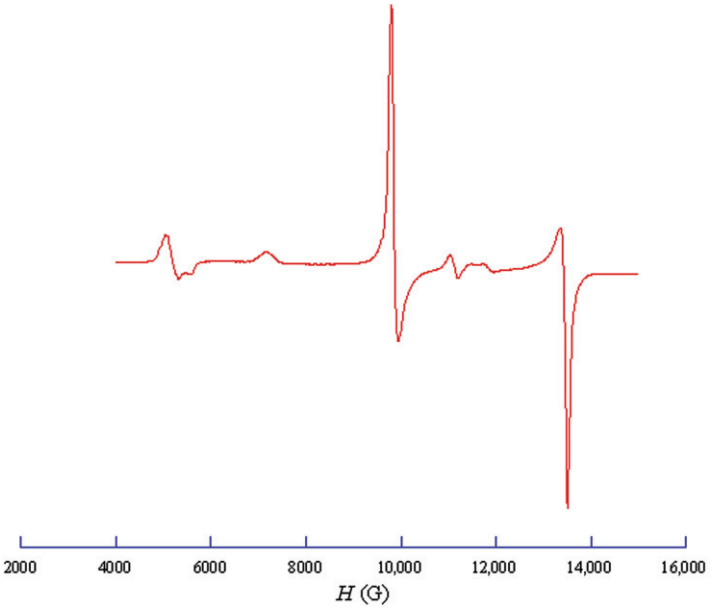

Figure 7. EPR Q band ($\nu = 34.0289$ GHz) spectrum of powdered **5** at 120 K.

Powder EPR spectra of **1**, **3**, **5**, **6**, and **7**, at Q band and at 120 K show signals of the triplet state ($S = 1$) for $D \neq 0$ and $E \approx 0$, due to the presence of the dimeric units. Figure 7 shows the spectrum of **5**.

The spectra were interpreted according to the Wasserman, Snyder, and Yager equations [25] based on the Hamiltonian $H = gHS\beta + D[S_z^2 - 2/3] + E[S_x^2 - S_y^2]$, with $D \neq 0$ and $E = 0$.

For $\Delta M = \pm 1$:

$$H_{\parallel} = (g_e/g_{\parallel})(H_o - D')$$

$$H_{\perp 1} = (g_e/g_{\perp})[H_o(H_o - D')]^{1/2}$$

$$H_{\perp 2} = (g_e/g_{\perp})[H_o(H_o + D')]^{1/2}$$

For $\Delta M = \pm 2$:

$$H_{min} = (g_e/g_{min})[H_o^2/4 - D'^2/3)]^{1/2}$$

$$H_{dq} = (g_e/g_{av})[H_o^2 - D'^2/3]^{1/2}$$

$$H_o = h\nu/g_e\beta; \quad D' = D/g_e\beta$$

The experimental values of H and the calculated parameters: $g_{\parallel}$, $g_{\perp}$, g_{av}, and D are given in table 6.

Triplet state signals are often observed for antiferromagnetic copper pairs with the copper acetate *paddle-wheel* motif [25]. The magnetic moment values at 120 K (table 5) indicate significant occupation of the triplet state ($S = 1$) at this temperature.

Table 6. EPR results for **1**, **3**, **5**, **6**, and **7**.

Compound	H_{min} (G)	$H_{\parallel}$ (G)	$H_{\perp 1}$ (G)	$H_{\perp 2}$ (G)	H_{dq} (G)	$g_{\parallel}$	$g_{\perp}$	g_{av}	D (cm^{-1})
1	4910	6551	9300	13,837	11,754	2.31	2.07	2.15	0.43
3	5225	7350	9860	13,460	11,145	2.31	2.06	2.14	0.34
5	5150	7250	9795	13,510	11,120	2.31	2.06	2.14	0.35
6	5200	7350	9850	13,475	11,200	2.30	2.06	2.14	0.34
7	5220	7270	9850	13,460	11,145	2.31	2.06	2.14	0.34

4. Conclusions

By the reaction of methylpyrazine with $Cu(HCO_2)_2 \cdot 4H_2O$ and $Cu(AcO)_2 \cdot H_2O$, compounds of composition $\{[Cu_2(\mu\text{-}HCO_2)_4](\mu\text{-Mepyrz})\}_n$ (**1**) and $\{[Cu_2(\mu\text{-AcO})_4](\mu\text{-Mepyrz})\}_n$ (**3**) are obtained only in the powder form. Crystals suitable for X-ray diffraction for the molecular dimers $[Cu_2(\mu\text{-}HCO_2)_4(Mepyrz)_2]$ (**2**) and $[Cu_2(\mu\text{-AcO})_4(Mepyrz)_2]$ (**4**), in which the methylpyrazine is coordinated through one of the two nitrogens, are obtained. With 2,6-Me_2pyrz, only $[Cu_2(\mu\text{-AcO})_4(2,6\text{-}Me_2pyrz)_2]$ is obtained. The 2,6-Me_2pyrz is monodentate due to the steric effect of the two methyl groups. The difference between the behavior of 2,3-Me_2pyrz (monodentate in **5**) and 2,5-Me_2pyrz (bridging bidentate in **7**) is more difficult to explain. In the formate compound, $Cu_2(HCO_2)_4(2,3\text{-}Me_2pyrz)$ [9], the structure is of a chain of dimeric units of $Cu_2(HCO_2)_4$ linked by bridging 2,3-Me_2pyrz.

In all the structures studied, the dimeric units have structural characteristics similar to those found in *paddle-wheel* Cu(II) compounds.

The magnetic measurements correspond to the antiferromagnetic effect of *paddle-wheel* $[Cu_2(\mu\text{-RCOO})_4]$ units. In EPR spectra, the signals of triplet state ($S = 1$) for $D \neq 0$ and $E \approx 0$ are observed. The magnetic and EPR results suggest a chain structure in **1** and **3**, similar to that of **7**.

Supplementary material

CCDC-256040 and 740813–780416 contain the supplementary crystallographic data for **2** and **4**–**7**, respectively. These data can be obtained free of charge from the Cambridge Crystallographic Data Centre (CCDC) *via* www.ccdc.cam.ac.uk/data_request/cif.

Acknowledgments

This work was supported by the "Diputación Foral de Gipuzkoa" in a program co-financed by the European Union (FEDER).

References

[1] P. De Mester, S.R. Fletcher, A.C. Skapski. *J. Chem. Soc., Dalton Trans*., 2575 (1973).
[2] R.L. Carlin. *Magnetochemistry*, Springer, Berlin-Heidelberg (1986).
[3] J. Catterick, P. Thornton. *Adv. Inorg. Chem. Radiochem*., **20**, 291 (1977).
[4] R.J. Doednes. *Prog. Inorg. Chem*., **21**, 209 (1976).
[5] V.M. Rao, D.N. Sathyanarayana, H. Manohar. *J. Chem. Soc., Dalton Trans*., 2167 (1983).
[6] M. Nakagawa, Y. Inomata, F.S. Howell. *Inorg. Chim. Acta*, **295**, 121 (1999).
[7] D.B.W. Yawney, R.J. Doedens. *Inorg. Chem*., **9**, 1626 (1970).
[8] F. Sapiña, M. Burgos, E. Escrivá, J.V. Folgado, D. Beltrán, P. Gómez-Romero. *Inorg. Chim. Acta*, **216**, 185 (1994).
[9] R. Cejudo, G. Alzuet, J. Borrás, M. Liu-González, F. Sanz-Ruiz. *Polyhedron*, **21**, 1057 (2002).
[10] M. Bukowska-Strzyzewska. *Roczniki Chem*., **40**, 567 (1966).
[11] J.M. Seco, M.J. González Garmendia, E. Pinilla, M.R. Torres. *Polyhedron*, **21**, 457 (2002).
[12] M. Barquín, M.J. González Garmendia, S. Pacheco, E. Pinilla, S. Quintela, J.M. Seco, M.R. Torres. *Inorg. Chim. Acta*, **357**, 3230 (2004).
[13] M. Barquín, M.J. González Garmendia, L. Larrínaga, E. Pinilla, M.R. Torres. *Inorg. Chim. Acta*, **359**, 2424 (2006).
[14] R. Sarma, J.B. Baruah. *J. Coord. Chem*., **61**, 3329 (2008).
[15] M.J. González Garmendia, V. San Nancianceno, J.M. Seco, F.J. Zúñiga. *Acta Crystallogr., Sect. C*, **65**, m436 (2009).
[16] T. Otieno, A.R. Hutchison, M.K. Krepps, D.A. Atwood. *J. Chem. Educ*., **79**, 1355 (2002).
[17] J.S. Valentine, A.J. Silverstein, Z.G. Soos. *J. Am. Chem. Soc*., **96**, 97 (1974).
[18] B. Morosin, R.C. Hughes, Z.G. Soos. *Acta Crystallogr., Sect. B*, **31**, 762 (1975).
[19] M. Barquín, M.J. González Garmendia, L. Larrínaga, E. Pinilla, M.R. Torres. *Z. Anorg. Allg. Chem*., **631**, 2210 (2005).
[20] Ch.J. O'Connor. *Prog. Inorg. Chem*., **29**, 203 (1982).
[21] G.M. Sheldrick. *SHELX-97, Program for Refinement of Crystal Structure*, University of Göttingen, Göttingen, Germany (1997).
[22] A.W. Addison, T.N. Rao, J. Reedjik, J. Van Rijn, G.C. Verschoor. *J. Chem. Soc., Dalton Trans*., 1349 (1984).
[23] M. Nakashima, M. Mikuriya, Y. Muto. *Bull. Chem. Soc. Jpn*, **58**, 968 (1985).
[24] A. Rodríguez-Fortea, P. Alemany, S. Alvarez, E. Ruiz. *Chem. Eur. J*., **7**, 627 (2001).
[25] A. Bencini, D. Gatteschi. *EPR of Exchange Coupled Systems*, p. 174, Springer, Berlín (1990).